Earth and Planetary Science Letters 493 (2018) 47–56

Contents lists available at ScienceDirect

Earth and Planetary Science Letters

www.elsevier.com/locate/epsl

Progressive reactivation of the volcanic plumbing system beneath Tolbachik volcano (Kamchatka, Russia) revealed by long-period seismicity

William B. Frank [a,b,*], Nikolaï M. Shapiro [c,d], Alexander A. Gusev [e]

[a] Department of Earth, Atmospheric, and Planetary Sciences, Massachusetts Institute of Technology, Cambridge, MA 02139, USA
[b] Department of Earth Sciences, University of Southern California, Los Angeles, CA 90089-0740, USA
[c] Institut de Physique du Globe de Paris, UMR CNRS 7154, Paris, France
[d] Schmidt Institute of Physics of the Earth, Russian Academy of Sciences, Moscow, Russia
[e] Institute of Volcanology and Seismology FEB RAS, Petropavlovsk-Kamchatsky 683006, Russia

A R T I C L E I N F O

Article history:
Received 6 November 2017
Received in revised form 11 April 2018
Accepted 12 April 2018
Available online xxxx
Editor: P. Shearer

Keywords:
eruptive cycle
long-period earthquakes
volcanic plumbing system
point process

A B S T R A C T

After lying dormant for 36 yr, the Tolbachik volcano of the Klyuchevskoy group started to erupt on 27 November 2012. We investigate the preparatory phase of this eruption via a statistical analysis of the temporal behavior of long-period (LP) earthquakes that occurred beneath this volcanic system. The LP seismicity occurs close to the surface beneath the main volcanic edifices and at 30 km depth in the vicinity of a deep magmatic reservoir. The deep LP earthquakes and those beneath the Klyuchevskoy volcano occur quasi-periodically, while the LP earthquakes beneath Tolbachik are clustered in time. As the seismicity rate increased beneath Tolbachik days before the eruption, the level of the time clustering decreased. We interpret this as a manifestation of the evolution of the volcano plumbing system. We suggest that when a plumbing system awakes after quiescence, multiple cracks and channels are reactivated simultaneously and their interaction results in the strong time clustering of LP earthquakes. With time, this network of channels and cracks evolves into a more stable state with an overall increased permeability, where fluids flow uninhibited throughout the plumbing system except for a few remaining impediments that continue to generate seismic radiation. The inter-seismic source interaction and the level of earthquake time clustering in this latter state is weak. This scenario suggests that the observed evolution of the statistical behavior of the shallow LP seismicity beneath Tolbachik is an indicator of the reactivation and consolidation of the near-surface plumbing system prior to the Tolbachik eruption. The parts of the plumbing system above the deep magmatic reservoir and beneath the Klyuchevskoy volcano remain in nearly permanent activity, as demonstrated by the continuous occurrence of the deep LP earthquakes and very frequent Klyuchevskoy eruptions. This implies that these parts of the plumbing system remain in a stable permeable state and contain a few weakly interacting seismogenic sources. Our results provide new constraints on future mechanical models of the magmatic plumbing systems and demonstrate that the level of time clustering of LP earthquakes can be a useful parameter to infer information about the state of the plumbing system.

1. Introduction

Seismicity is one of the main observable manifestations of volcanic unrest (e.g. Chouet, 2003; McNutt, 2005; Sparks et al., 2012; Chouet and Matoza, 2013). Most pre- and co-eruptive processes within volcanic systems are accompanied by seismic radiation that can be used to detect and identify different phases of the eruptive cycle. Seismic signals associated with volcanic unrest take many forms. Stresses induced by the ascending magma are released in the form of volcano-tectonic earthquakes (e.g. Roman and Cashman, 2006). Magmatic and hydrothermal volcanic systems also generate earthquakes and tremors with periods that are longer than those for typical tectonic earthquakes of similar sizes (e.g. Fehler, 1983; Chouet, 1988, 1996; Iverson et al., 2006). The mechanisms involved in the generation of this long-period (LP) seismicity are often believed to be different from those of tectonic earthquakes (Chouet, 1996). LP earthquakes are commonly inter-

* Corresponding author at: Department of Earth Sciences, University of Southern California, Los Angeles, CA 90089-0740, USA.
E-mail address: wbfrank@usc.edu (W.B. Frank).

https://doi.org/10.1016/j.epsl.2018.04.018
0012-821X/

preted as reflecting pressure fluctuations within magmatic and hydrothermal fluids, and are considered a reliable precursor of volcanic eruptions (e.g. Chouet, 1988, 1996; Chouet and Matoza, 2013; Power et al., 2013). Possible triggering mechanisms include magma-hydrothermal interactions (Waite et al., 2008) and magmatic degassing (Ripepe et al., 1996; Lees et al., 2004; Jolly et al., 2017). Other studies have proposed mechanisms such as brittle fractures of melt and near-vent plug stick-slip (e.g Iverson et al., 2006; Neuberg et al., 2006; Kendrick et al., 2014) and crack opening during deformation of the volcanic edifice (Bean et al., 2014). Most of reported volcanic LP seismicity reflects the activity within shallow magmatic reservoirs and hydrothermal systems. In this context, volcanic deep LP earthquakes (e.g. White, 1996; Nakamichi et al., 2003; Power et al., 2004; Nichols et al., 2011; Shapiro et al., 2017a; Han et al., 2018) that occur in the lower crust and the uppermost mantle are particularly interesting, because they reflect the pressurization of deep-seated parts of the magmatic systems and the transfer of magma and pressure toward the surface.

Volcanic LP earthquakes are known to occur in bursts and are often associated with volcanic tremors (Fehler, 1983; Chouet, 1996). Shaw and Chouet (1991) used a statistical analysis of tremor to characterize the magma transport system beneath Hawaii. In our study, we use a statistical analysis of the LP earthquake catalogs to extract information about the complexity of the different parts of the plumbing system through which fluids are transported. We use the approach of Frank et al. (2016) to infer the level of time clustering of LP earthquakes. We argue that this clustering depends on the level of interaction between different seismic sources and reflects the level of connectivity of the underlying fluid transport system.

2. Klyuchevskoy volcanic group

We analyze here catalogs of deep and shallow LP earthquakes that occurred within the Klyuchevskoy volcano group (KVG) in Kamchatka, Russia (Fig. 1a) during 2011 and 2012 (Shapiro et al., 2017a). The KVG is one of the largest and most active clusters of subduction zone volcanoes in the world (e.g. Fedotov et al., 1987, 2010; Koulakov et al., 2011, 2017; Churikova et al., 2013; Ozerov et al., 2013; Bergal-Kuvikas, 2015; Shapiro et al., 2017b). The KVG is located above the edge of the Pacific plate at the Kamchatka–Aleutian junction where the Hawaii-Emperor Seamount chain is subducted. Possible explanations of the exceptionally active KVG include fluid being released from the thick, highly hydrated Hawaii-Emperor Seamount crust (Dorendorf et al., 2000), mantle flow around the corner of the Pacific plate (Yogodzinski et al., 2001), and a recent detachment of a portion of the subducting slab (Levin et al., 2002). The KVG contains 13 large stratovolcanoes, three of which (Klyuchevskoy, Bezymianny, and Tolbachik) have erupted during recent decades.

The abundant seismic activity of the KVG volcanoes includes extended periods of tremor and numerous volcano-tectonic and LP earthquakes. The most prominent source of LP seismicity is located at approximately 30 km depth just below the Moho beneath Klyuchevskoy and is associated with the deep-seated magmatic reservoir (Levin et al., 2014). These deep LP earthquakes have occurred nearly continuously since seismological observations begun at the KVG (Gorelchik et al., 2004; Senyukov et al., 2009; Senyukov, 2013; Shapiro et al., 2017a). Shallow bursts of LP earthquakes and tremor episodes are associated with the unrest of the three active volcanoes (e.g. Gordeev et al., 1986; Senyukov et al., 2009; Thelen et al., 2010; Senyukov, 2013; Droznin et al., 2015; Soubestre et al., 2018), with the most frequent seismic and volcanic activity beneath Klyuchevskoy.

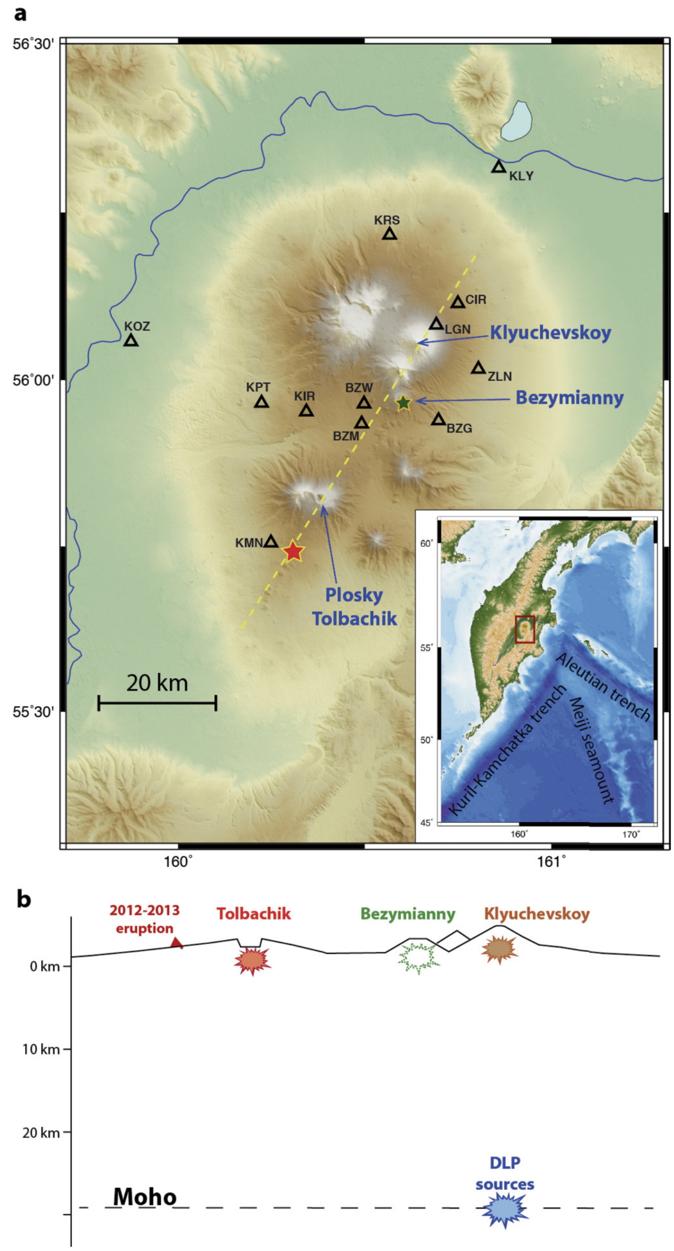

Fig. 1. (a) Map of the Klyuchevskoy volcano group. The inset shows the general geographical and tectonic settings. Triangles show the positions of the seismic stations. The recently active volcanoes are indicated with blue arrows. The red star shows the eruptive center of the 2012–2013 Tolbachik eruption. (b) Cross-section along the profile indicated in (a) by the yellow dashed line, showing a schematic representation of the KVG plumbing system and the locations of the four groups of LP sources. We do not analyze the shallow seismicity beneath Bezymianny in this study. (For interpretation of the colors in the figure(s), the reader is referred to the web version of this article.)

In this study we focus on the KVG LP seismic activity preceding the most recent eruption of Tolbachick, which started on 27 November 2012 and continued until September 2013 (e.g. Gordeev et al., 2013; Belousov et al., 2015; Kugaenko et al., 2015; Senyukov et al., 2015). Previous reported eruptions of this volcano have occurred in 1740, 1941, and 1975–1976 (Gordeev et al., 2013). The 2012–2013 eruption occurred after 36 yr of quiescence at Tolbachik and constitutes a major unrest event of the past 20 yr at the KVG. The analysis of seismicity during the pre-eruptive period provides an opportunity to investigate the processes that were involved in the re-activation of the Tolbachik plumbing system.

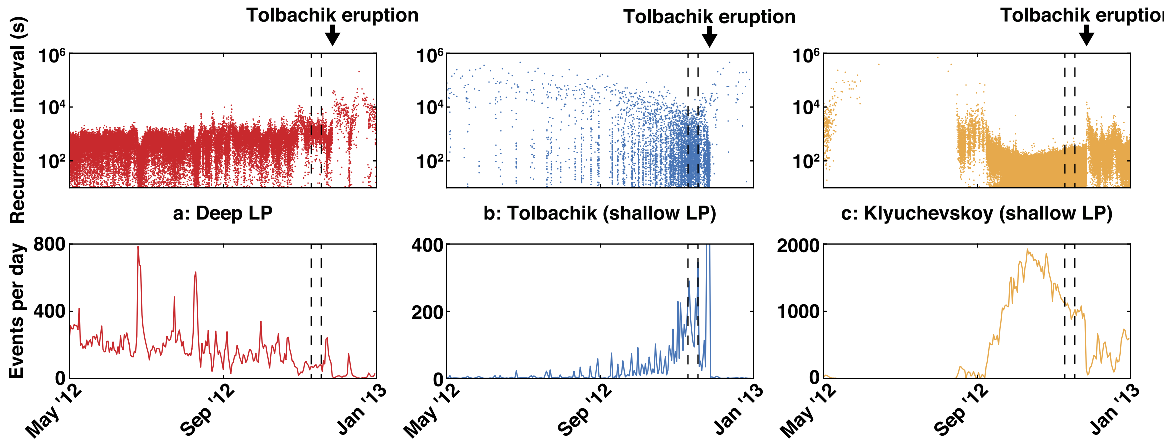

Fig. 2. Occurrence of LP earthquakes in three different source regions between 16 March and 30 November 2012: (a) deep LP events, (b) shallow Tolbachik LP events, and (c) shallow Klyuchevskoy LP events. Upper and lower frames show inter-event times and daily event counts, respectively. The dashed boxes indicate the eight day period analyzed in Figs. 4 and 5. Note the y-axis of the bottom panels is different for each volcano. The event count plot for Tolbachik is saturated and the maximum value reached on the day preceding the eruption is 2,242.

3. Detection of LP earthquakes beneath the Klyuchevskoy volcano group

The activity of KVG is monitored by a seismic network that is operated by the Kamchatka Branch of the Geophysical Survey of the Russian Academy of Sciences (Chebrov et al., 2013; Senyukov, 2013). Positions of the twelve stations that recorded the LP activity analyzed here are plotted in Fig. 1a. We analyzed the LP catalogs from Shapiro et al. (2017a); see reference for further details such as detection and correlation thresholds. The main property of the detected LP earthquakes is their multiplet behavior with many events generated by repetitive sources (Matoza and Chouet, 2010). In the first step of the detection procedure, continuous seismograms were bandpassed filtered between 1 and 5 Hz. The continuous vertical component records at individual stations from 2012 were analyzed to find all time windows with elevated signal-to-noise ratios. Templates were then identified as events that showed significant similarity across this ensemble of energetic signals. These one-component templates were used for initial matched-filter detection of the repeated events (Gibbons and Ringdal, 2006; Frank et al., 2014). The waveforms for all detections from the same template at all stations and three components were stacked to form the final multi-component templates that were used to pick the arrival times of P-waves and S-waves and to locate the sources of the multiplet families. The final matched-filter detection was then executed with these multi-component templates. Overall, 12 families (templates) of LP earthquakes were identified that were regrouped into four source regions (Fig. 1b). The deep LP source region is located at ∼30 km depth beneath Klyuchevskoy, above the assumed subcrustal magma reservoir (Levin et al., 2014), and the remaining sources are located near the surface, below the active KVG volcanoes.

4. Temporal distribution of long-period seismicity prior to the Tolbachik eruption

The LP activity from May to the end of November 2012 are shown in Fig. 2 (the LP seismic crisis beneath Bezymianny is not shown because it was too short to be used in our analysis). As described in Shapiro et al. (2017a), the activity in the deep LP source started to increase in late March 2012, and in May reached its average maximum level. During the considered period, the rate of deep LP events is on average decreasing, except for a few short bursts of activity. The shallow seismicity beneath Tolbachik instead presents a steadily increasing rate of seismicity until the 27 November eruption. The shallow source beneath Klyuchevskoy was inactive until September and exhibited a very intense activity during the 2.5 months prior to the Tolbachik eruption.

A closer look at the shallow seismicity beneath Tolbachik (see Figs. 2 and 3) shows that the number of events does not increase smoothly but is rather characterized by a stepped evolution, similar to other volcanoes (e.g. Matoza et al., 2014) and indicative of a clustered event distribution in time (Frank et al., 2016). Plotting the recurrence intervals (or interevent times) of the three seismic sources over an 8-day period in Fig. 4, we clearly observe the bursty nature of the Tolbachik seismicity compared to the constant stream of deep LP earthquakes and the activity beneath Klyuchevskoy.

We use the method proposed by Frank et al. (2016) who studied similar clusters of low-frequency seismicity, but in the context of slow slip along the Mexican subduction zone in Guerrero. This approach is based on statistical tools, which we describe below, to analyze each LP seismic source as a point process (Lowen and Teich, 2005).

4.1. Clustered shallow LP earthquakes beneath Tolbachik

Each seismic source (shallow and deep) can be considered as a discrete point process that generates events whose timing is controlled by some underlying statistical distribution. In such a framework, it is possible to quantify the temporal correlation, or clustering, of event times (Frank et al., 2016). We first generate the event count time series for each seismic source from May 2012 to December 2012, defined as the histogram of event counts within 1-minute time bins. With the seismic source discretized as a regularly sampled time series, we compute the autocorrelation of the event count time series. An event count autocorrelation represented by a zero-lag delta function is indicative of a random Poisson distribution of events, while a smooth falloff from zero lag suggests that there are short term correlations and clustering of the events (see Fig. A1 for an example) (Lowen and Teich, 2005; Frank et al., 2016). In many cases, this clustering is scale-invariant (and therefore fractal). The level of clustering can then be quantified as the exponent α of the underlying power-law distribution of event recurrence intervals (Lowen and Teich, 2005), which manifests itself as the linear slope of the power spectrum of event count time series in log–log space. If instead the event count power spectrum on a log–log scale is nearly constant (slope of zero), then the power-law exponent α is zero and could reflect a Poisson point process. In any case, the scale-invariant (fractal) model of event

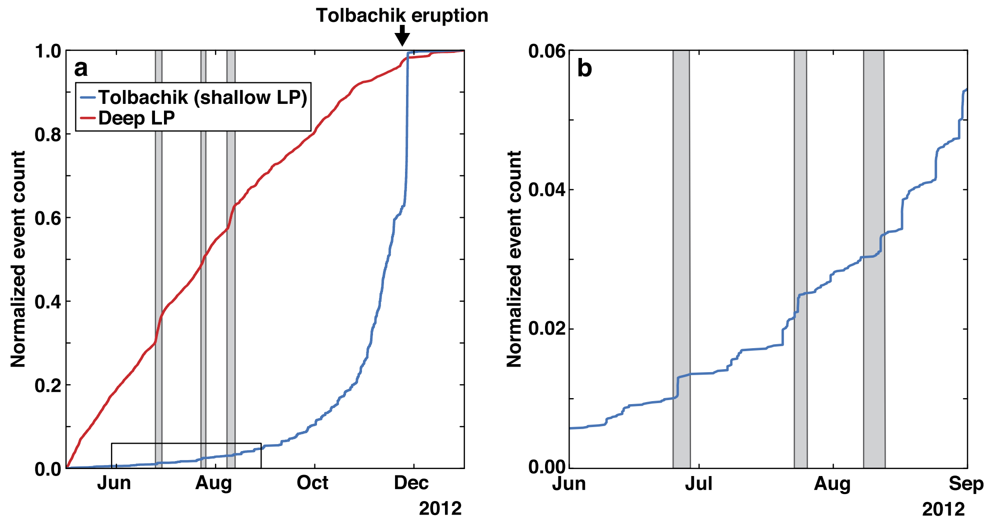

Fig. 3. Normalized cumulative event count of shallow Tolbachik (blue) and deep (red) LP seismicity beneath Tolbachik. The shaded gray boxes indicate increases of activity of the deep LP earthquakes. The thin black box indicates the area of the zoom shown in (b), which highlights the step-like evolution of shallow LP seismicity that is suggestive of clustered event distributions (Frank et al., 2016).

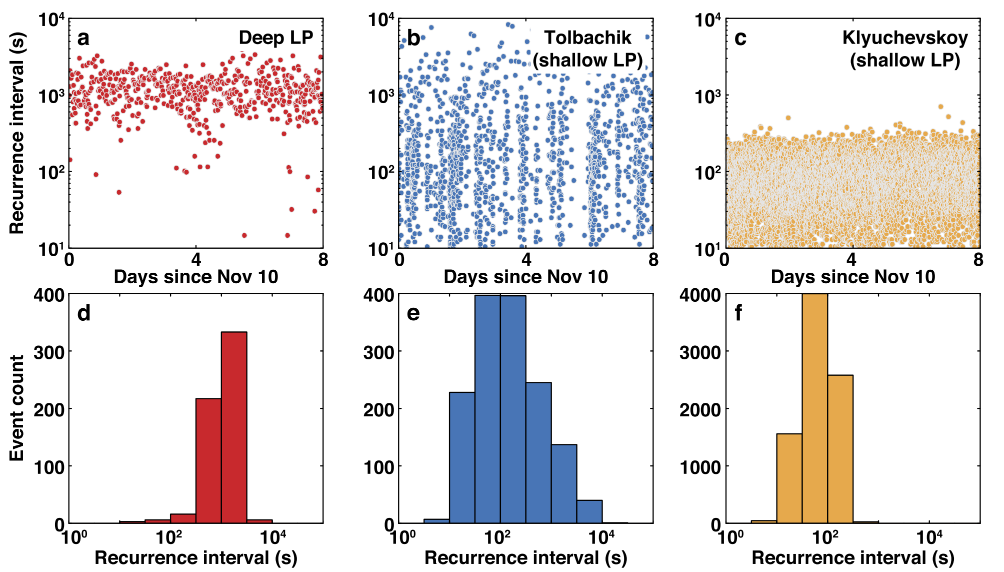

Fig. 4. Distribution of recurrence intervals during an eight day period (10–18 November 2012), nine days prior to eruption. The top panels (a–c) show recurrence intervals in time while the bottom panels (d–f) show the histograms of those recurrence intervals. The shallow LP seismicity beneath Tolbachik (blue) is organized in distinct clusters of seismicity while the deep LP seismicity (red) and shallow LP events beneath Klyuchevskoy (orange) exhibit a more regular event timing.

clustering is not applicable when $\alpha = 0$. The power law exponent α can then be determined as the linearly regressed slope of the power spectrum.

To illustrate this process, we analyze in Fig. 5 the shallow seismicity beneath Tolbachik during an eight-day period two weeks prior to the 27 November Tolbachik eruption. We first observe a stepped cumulative event count that is different from the smoother cumulative event count of a synthetic Poisson event catalog. We then process the event count time series of the Tolbachik LP seismicity to compute its autocorrelation (Fig. A1) and power spectrum. We find a distinct (log–log) linear slope of $\alpha = 0.32$ in Fig. 5b that indicates a scale-invariant clustering of Tolbachik LP earthquakes; the slope of the synthetic Poisson catalog is $\alpha = 0$ as expected. A jackknife analysis is then performed to evaluate the robustness our estimation of α. We randomly resample 90% of the events within the analyzed time window and estimate α again via the method described above; given the scale invariant nature of the clustering, α should not change with a smaller sampling of the same event distribution. After resampling 1,000 times, we determine respectively a final estimate of the clustering exponent α and its uncertainty as the mean and the standard deviation of the distribution shown in Fig. A2.

4.2. Quasi-periodic occurrence of deep LP earthquakes

Now considering the distribution of deep LP earthquakes in Fig. 5, we observe a near constant event rate as evidenced by a smooth linear cumulative event count that resembles the synthetic Poisson event catalog. If, however, we apply the above processing to this deep seismicity, we observe neither a power spectrum with a linear increase in log–log space that would be associated with a clustered scale-invariant point process, nor a flat spectrum that could reflect a Poisson point process. We instead observe in Fig. 5b a flat event count power spectrum that has a vertical offset at a period of about 30 min. We suggest that the assumption of a scale-invariant (fractal) point process is invalid for the deep LP activity, and cannot be characterized by the clustering exponent α. To quantify this activity, we instead use the coefficient

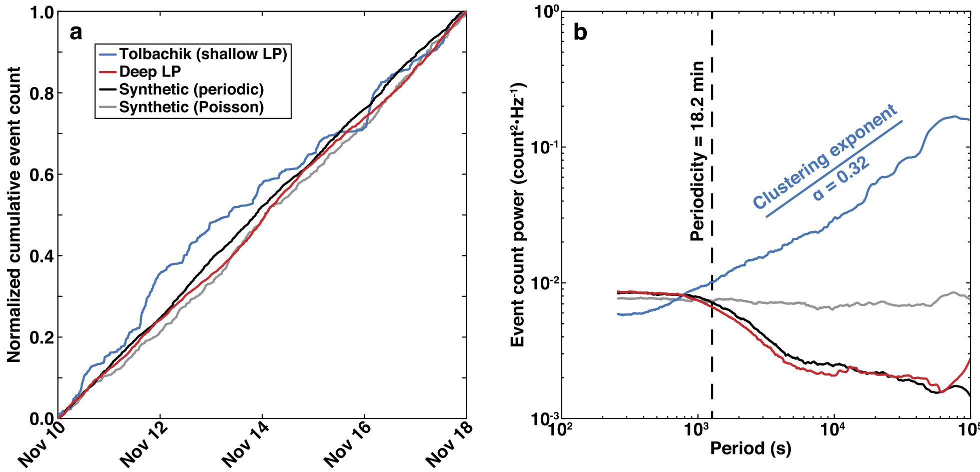

Fig. 5. Comparing the different temporal distributions of deep and shallow LP seismicity. Both deep and shallow Tolbachik LP seismicity is analyzed during the same time period shown in Fig. 4, 10–18 November 2012. (a) Normalized cumulative event counts of LP seismicity compared to quasi-periodic (black) and Poisson (gray) synthetic catalogs. (b) Event count power spectra for the four catalogs plotted in (a). The 18.2 min periodicity of the quasi-periodic catalog (dashed black line) is defined as the median of the deep seismicity's recurrence intervals in Fig. 4. While the cumulative event counts of the Poisson and the quasi-periodic synthetic catalogs are indistinguishable, their event count spectra are distinct and the quasi-periodic catalog best reproduces the observed event count spectrum of the deep LP seismicity.

Table 1
Coefficient of variation (COV) computed for various long-period (LP) source regions. The first three rows present the COV computed for the time window analyzed for Figs. 4 and 5: 10–18 November 2012. The final row for Tolbachik is computed during the last 12 h prior to eruption (Fig. 7).

LP source	COV	# of events	Start	Duration (days)
Deep	0.53	581	10 Nov 2012 00:00UTC	8
Tolbachik (shallow)	2.20	1451	10 Nov 2012 00:00UTC	8
Klyuchevskoy (shallow)	0.74	8204	10 Nov 2012 00:00UTC	8
Tolbachik eruption (shallow)	0.57	1700	26 Nov 2012 15:00UTC	0.5

of variation (COV), defined as the standard deviation of the recurrence intervals divided by their mean; a value of 0 indicates a perfectly periodic process, a value of 1 indicates a random Poisson process, and a value ≥ 2 indicates a time clustered process (e.g. Sicali et al., 2014). Table 1 presents the COV computed for the shallow LP events beneath Tolbachik and Klyuchevskoy and the deep LP events during the time period shown in Figs. 4 and 5. We observe COV values between 0 and 1 for both shallow LP earthquakes beneath Klyuchevskoy and deep LP events, suggesting some degree of periodicity; the obtained COV for Tolbachik is in agreement with our observations that the shallow LP seismicity there is clustered in time. Taking into account the low COV values, the observed near constant event rate, and a narrower distribution of recurrence intervals compared to the Tolbachik LP earthquakes (Fig. 4), we propose that the distribution of deep LP earthquakes reflects a quasi-periodic point process.

We produce a quasi-periodic synthetic catalog, whose cumulative event count is shown in Fig. 5, to model the deep LP seismicity as a point process whose event recurrence intervals (waiting times) are drawn from a Gaussian distribution. The mean and the standard deviation of this normal distribution are respectively set as the median ($\sim$18.2 min) and the standard deviation ($\sim$10.6 min) of the deep LP recurrence intervals (Fig. 4) during the 8-day window. We use the median instead of the mean because the distribution of observed recurrence intervals resembles a truncated Gaussian (see Fig. A3). This truncation results from the minimum time between two events, which is defined as 9.375 s, a quarter of the detecting earthquake template duration (Shapiro et al., 2017a). We impose this same minimum recurrence interval on the synthetic catalog. To generate the synthetic event catalog, we draw the same number of events from this truncated Gaussian distribution as there are deep LP earthquakes during the 8-day period (581). We finally impose that the duration of the synthetic catalog must be similar to the analyzed 8-day time window (no less than one tenth of a day shorter or longer).

Comparing a representative synthetic catalog to the deep seismicity catalog, we find that our quasi-periodic point process model is able to reproduce both the event count power spectrum in Fig. 5b (and consequently the event count autocorrelation seen in Fig. A1) and the observed distribution of recurrence intervals (Fig. A3). We perform this comparison during different periods with time windows of varying length and observe similar quasi-periodic event distributions prior to the Tolbachik eruption during 2011, albeit with different median recurrence intervals. From this result, we suggest a quasi-periodic source reproduces well the timing of deep LP seismicity. While quasi-periodic, we note that the deep LP activity is not as distinctly periodic as volcanic drumbeat seismicity (e.g. Iverson et al., 2006; Moran et al., 2008; Matoza and Chouet, 2010).

4.3. Activity of shallow long-period earthquakes beneath Klyuchevskoy

The shallow LP activity beneath Klyuchevskoy from September 2012 until the Tolbachik eruption is extremely intense as shown in Figs. 2 and 4, much more so than either the deep LP seismicity or the shallow LP activity beneath Tolbachik. Because of the high event rates and the minimum time between sequential events of 9.375 s, the catalog of LP earthquakes beneath Klyuchevskoy is saturated and presents a statistically biased distribution of event timings. The computed COV of 0.74 for the Klyuchevskoy LP seismicity is similar to the quasi-periodic deep LP seismicity (Table 1). Taking this into account along with a similar narrow distribution of recurrence intervals compared to the deep LP source (Fig. 4), we suggest that the Klyuchevskoy LP earthquakes are also best characterized by a quasi-periodic event timing.

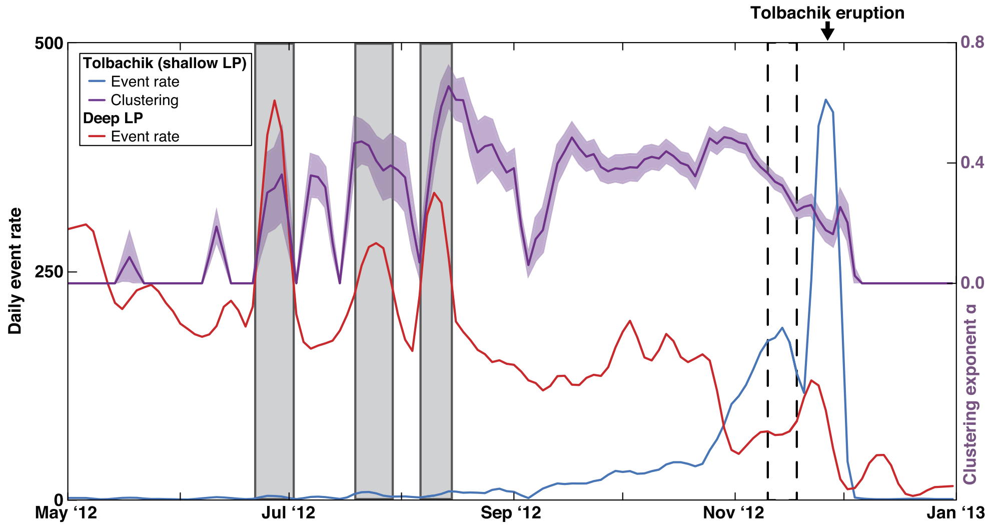

Fig. 6. Evolution of deep and shallow LP earthquake activity leading up to the November 2012 eruption of Tolbachik. The event rates for both shallow (beneath Tolbachik; blue) and deep (beneath Klyuchevskoy; red) LP seismicity are plotted on the left axis. The right axis tracks the clustering exponent α of the shallow LP earthquakes in purple; the shaded region represents the estimated 2σ uncertainty (see Fig. A4). The dashed box indicates the 8-day period shown in Fig. 4 and analyzed in Fig. 5. Increased deep activity highlighted by grey patches is well correlated with increased clustering within the shallow LP earthquakes that is not otherwise visible in the event rate. This clustering gradually disappears as shallow LP seismicity abruptly increases prior to eruption.

5. Monitoring the preparatory phase of eruption with long-period earthquakes

We use the above statistical characterizations of the LP earthquakes sources to track the evolution of the preparatory phase of the Tolbachik eruption in Fig. 6. In a sliding 8-day window with a 75% overlap, we compute three quantities: the event rate and the clustering exponent α for the shallow seismicity beneath Tolbachik, and the event rate for the deep LP source. We chose an 8-day duration to capture the evolution of the α as it varies in time, while still being able to observe longer periods. We use the strategy described in section 4.1 to estimate α and its uncertainty; no estimation of α is made for time windows that contain less than 20 events. The estimated uncertainty of the clustering exponent α is never greater than 0.1, as shown in Fig. A4.

We observe a clustering of shallow Tolbachik LP seismicity that steadily increases in July and August, despite relatively low and stagnant event rates, before reaching a high in September and October. The three highest levels of Tolbachik event clustering prior to eruption (highlighted in Figs. 3 and 6) occur shortly after heightened periods of deep seismic activity. This suggests that we can constrain the timing of the ascension of magmatic fluids via the temporal distribution of LP seismicity. While there is a fluctuation of the shallow event rate concurrent with the observed increase of clustering, we remark that the relative change in event rate is much smaller than the increase in clustering. This qualitative correlation between deep activity and the clustering of the Tolbachik seismicity corroborates recent work that suggests magma sources at different depths are linked by upward fluid transfer, a potential driver of LP earthquakes (Shapiro et al., 2017a).

After remaining steady for two months, there is then a clear decrease in the clustering of the Tolbachik seismicity that starts a month prior to eruption (Fig. 6). This decrease is coincident with an increase of the event rate. Looking at a two-day snapshot before the Tolbachik eruption of the shallow LP activity recurrence intervals in Fig. 7, we see that the distinguishing feature of the seismicity shifts from clustered event bursts to a dense swarm of LP earthquakes. This result shows that the clustering exponent α is able to capture this change in behavior of the shallow Tolbachik LP seismicity.

6. Reactivation of the volcanic plumbing system beneath Tolbachik

The observed LP seismicity reflects the pre-eruptive changes in the plumbing system. The shallow part of this system beneath Tolbachik has been sealed during the 36 yr that the volcano has lain dormant. As described by Shapiro et al. (2017a), this eruption was initially preceded by an increase of the deep LP activity, likely reflecting the pressurization of the deep magmatic reservoir. In mid 2012, this activity started to migrate toward the surface and the first manifestations of reactivation of the shallow plumbing system beneath Tolbachik appeared in May (Fig. 2). The shallow LP activity increased until the 27 November eruption, reflecting the progressive opening of the network of conduits and fractures (e.g., Hill, 1977; Shaw and Chouet, 1991) and its evolution towards a state of higher permeability.

The level of time clustering of the shallow LP events beneath Tolbachik (as measured by the exponent α) exhibits a pronounced evolution during the pre-eruptive crisis (Fig. 6). This time clustering is similar to the reported cascade behavior caused by interaction between low-frequency earthquakes (Frank et al., 2016), seismic events whose frequency content and strong link with high pore fluid pressure are similar to LP earthquakes (Shelly et al., 2006). We suggest that this interaction between seismic sources within the volcanic plumbing system is what we observe in Fig. 6 from June through October 2012, when the clustering of shallow seismicity increases. This increase in clustering is most clearly seen during periods of heightened activity of the deep LP seismic source, which we consider a proxy for the pressurization of the magma chamber at 30 km depth. The inferred interaction of LP seismicity within a fracture network also agrees with recent seismic crustal imaging beneath Tolbachik that highlights a complex fault network through which magma ascends (Koulakov et al., 2017).

Compared to the shallow LP earthquakes beneath Tolbachik, the statistical behavior of the deep LP earthquakes and the shallow LP events beneath Klyuchevskoy are very different. We do not observe time clustering in these two catalogs and instead the earthquakes occur quasi-periodically (Fig. 5b). This behavior could be explained by differences in permeability of the corresponding parts of the plumbing system. While the network of conduits be-

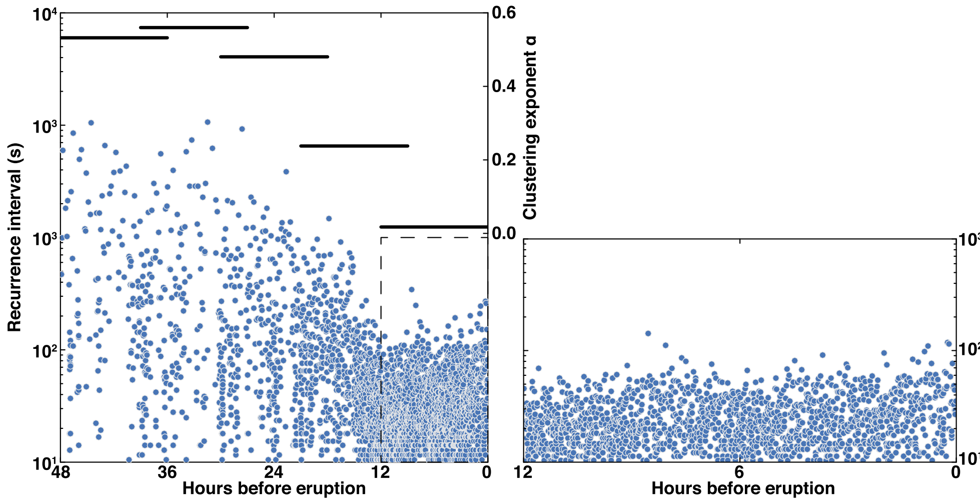

Fig. 7. Devolution of clustered LP seismicity beneath Tolbachik prior to eruption on 27 November 2012. The clustering exponent α measured in five 12 hr time windows (black lines) tracks a decreasing level of time clustering as the eruption approaches. During the 12 hr prior to eruption (zoom in right panel), the event distribution of seismicity changes regimes from one that is episodic and clustered to a quasi-periodic swarm of events similar to deep LP seismicity (Fig. 4).

neath Tolbachik progressively opens after being completely closed during 36 yr, the conduits above the deep magmatic reservoir and beneath Klyuchevskoy most likely do not remain sealed between episodes of volcanic unrest. This is confirmed by near-constant deep LP activity observed beneath Klyuchevskoy since the beginning of instrumental observations (Gorelchik et al., 2004; Senyukov et al., 2009), and by the very frequent eruptions of its volcanic edifice (e.g. Fedotov et al., 1987, 2010; Senyukov, 2013). We therefore suggest that the connectivity, or large-scale permeability, of the volcanic plumbing system between the deep magmatic source and Klyuchevskoy remains permanently elevated and magma is flowing though a network of inter-connected fluid pathways (Shapiro et al., 2017a).

The seismogenic processes in the quasi-open system below Klyuchevskoy is very different from the nearly sealed network of poorly connected conduits and fractures beneath Tolbachik. In the latter, many existing impediments for fluid flow result in the accumulation of significant pressure gradients, whose sudden release generates seismic radiation. We suggest that the build-up and spasmodic release of pressure creates a network of many closely located and interacting seismic sources that often act in cascades, resulting in a time clustering similar to our observations. In contrast, a network of well connected pathways would act as a either a single seismogenic source or a set of separate and non-interacting seismic sources. In both cases, the seismic sources would not cascade and would likely result in the quasi-periodic occurrence of earthquakes that is observed for the deep LP and the shallow Klyuchevskoy sources. Periodicities in both the ejection of volcanic material during eruptions and volcanic tremors, which represent the transfer of magma through seismically resonating conduits (Konstantinou and Schlindwein, 2003), are a common feature of volcanic plumbing systems (Ozerov et al., 2013). It is not surprising then that we are able to robustly characterize and reproduce the deep LP seismicity as a quasi-periodic source. This periodic activity suggests that the corresponding parts of the plumbing system steadily release accumulated fluid pressure, each release seismically manifesting as an LP earthquake. The observed variations in the seismicity rate likely correspond to variations in the rate of pressure build-up related to magma transport.

Our suggested inverse relationship between the level of the time clustering and the connectivity of the plumbing system is supported by the evolution of the shallow LP seismicity beneath Tolbachik during the month preceding the eruption. As the Tolbachik eruption approaches at the end of October 2012, the volcanic edifice is loaded with higher fluid pressures and magma from depth. During this process, the connectivity of the volcanic plumbing system should be enhanced to allow for magma transport, and would explain the observed progressive reduction of the clustering of seismicity (Fig. 6). We suggest that the devolution of organized clusters of LP earthquakes into an unorganized swarm of activity prior to eruption seen in Figs. 6 and 7 signals this consolidation of the volcanic plumbing system. The swarm of 1700 shallow LP earthquakes that lasted for about 12 hr (Fig. 7) is therefore the seismic signature of the last upward migration of magmatic fluid through the fully reactivated plumbing system before eruption. Analyzing the Tolbachik LP events during the last 12 hr prior to eruption, we find a COV of 0.57 that is suggestive of quasi-periodic behavior (Table 1); this is significantly different from the COV of 2.20 during the 8-day time window in Figs. 4 and 5. The visual similarity of shallow LP occurrence during the 12 hr before the Tolbachik eruption (Fig. 7) to the deep LP activity (Fig. 4) reinforces our interpretation that this swarm of activity represents magma transport driven by a quasi-periodic pressure source.

7. Conclusions

By treating catalogs of LP earthquakes as a point process, we constrain the underlying statistical distributions that govern the timing of seismicity beneath the Klyuchevskoy group of volcanoes during months preceding the November 2012 Tolbachik eruption. The periodic pressure release and upward transfer of fluid from the deep magma source at 30 km depth, as monitored by the quasi-periodic activity of deep LP earthquakes, loads the shallow magma source beneath the volcanic edifice. We compare the response of two separate regions of the shallow KVG plumbing system. We suggest that the one beneath Klyuchevskoy remains open because of the very frequent activity of this volcano, resulting in a quasi-periodic occurrence of the LP earthquakes that represents a steady release of the accumulated fluid pressure gradients modulated by the flux of the magma.

The observed response of the shallow plumbing system beneath Tolbachik is very different. It has remained sealed during 36 yr, and we suggest that its progressive opening initially creates a poorly connected network of conduits and fractures that behaves as an ensemble of interacting seismic sources, resulting in a strongly clustered timing of LP earthquakes. Moving closer to eruption after several months of reactivation, the interconnectivity and permeability of the Tolbachik volcanic plumbing system would then increase as the different fluid pathways consolidate.

This would be accompanied by a decrease of the inter-source interaction and a reduced level of time clustering, as we observe prior to the Tolbachik eruption. We suggest that the significant increase in shallow seismic activity 12 hr prior to eruption, without any signature of seismic source interaction, signals the last ascension of volcanic material through a consolidated magma conduit.

We conclude that through the novel analysis of seismicity catalogs, we are able to go beyond traditional seismic analysis of volcanoes, which is typically based on event rates and recurrence intervals. We show that the catalogs of volcanic earthquakes can be used to measure the level of time clustering, a quantitative parameter that is related to the level of connectivity of the network of conduits and fractures that comprise the plumbing system. The increase of this clustering in specific regions of the magmatic system is likely related to the opening of previously sealed fluid pathways. We interpret the consequent decrease of the level of clustering as a manifestation of the final pre-eruptive consolidation of the plumbing system beneath Tolbachik. The level of earthquake clustering therefore informs us about the state of the plumbing system and is a potential tool in eruption forecasting. Our characterization of LP seismicity through its time clustering and/or quasi-periodicity also provides important constraints on future mechanical models of the evolution of volcanic plumbing system throughout the eruptive cycle. Future work will extend this analysis to other types of volcanic seismicity to determine what other statistical signatures can be captured and studied to better understand volcanic eruption processes.

Acknowledgements

We thank all members of the Kamchatka Branch of the Geophysical Service of the Russian Academy of Sciences (http://www.emsd.ru) who contributed to the installation and maintenance of the Klyuchevskoy volcanic group seismic network, and to the collection and archiving of the data. This study was supported by the Russian Ministry of Education and Science of the Russian Federation (grant N 14.W03.31.0033) and by the French project "Labex UnivEarth" and the Université Sorbonne Paris Cité project "VolcanoDynamics". W.B.F. was supported by National Science Foundation grant EAR-PF 1452375.

Appendix

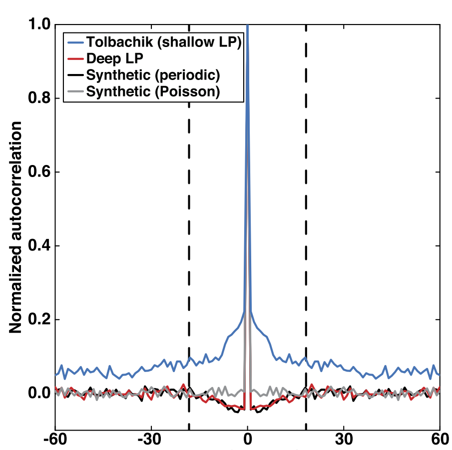

Fig. A1. Event count autocorrelation of deep and shallow Tolbachik LP seismicity and synthetic event catalogs. The shallow LP seismicity beneath Tolbachik (blue) exhibits short-term correlations indicative of clustered event timings, while the deep event count autocorrelation (red) is well reproduced by a quasi-periodic synthetic catalog (black). A Poisson synthetic catalog (gray) is not able to reproduce either observed catalog.

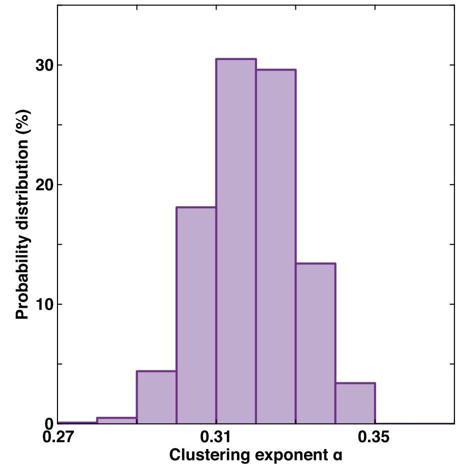

Fig. A2. Jackknifed distribution of the clustering exponent α of the shallow LP seismicity beneath Tolbachik during 10–18 November 2012. Ten percent of the 1452 events (145 events) are randomly removed before estimating the clustering exponent α following the method described in the main text; this jackknife sampling is performed 1,000 times. The clustering exponent α and its uncertainty are estimated as the mean and the standard deviation of the jackknifed distribution. The analyzed time period is the same shown in Figs. 4 and 5.

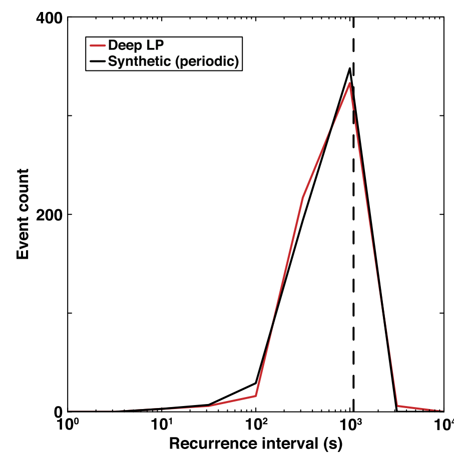

Fig. A3. Distribution of recurrence intervals for the deep LP earthquake catalog (red) during the 8-day period (Nov 10–18) in Fig. 5 and a quasi-periodic synthetic catalog (black). The dashed line highlights the estimated periodicity of 18.2 min.

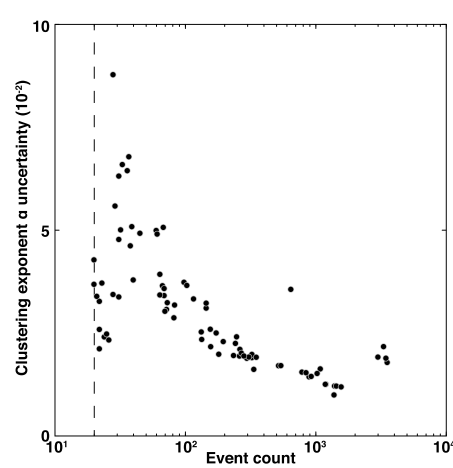

Fig. A4. Uncertainty of the clustering exponent α as a function of the number of analyzed events during the time period shown in Fig. 6. The dashed line indicates the minimum number of events needed in an eight-day time window to estimate α. The plotted uncertainty is the standard deviation of 1,000 jackknifed estimations of α, as shown in Fig. A2. The smallest numbers of events ($<\sim 30$) reflect non-clustered distributions whose clustering exponent is not significantly affected when removing events during the jackknife analysis.

References

Bean, C.J., De Barros, L., Lokmer, I., Métaxian, J.P., O'Brien, G.S., Murphy, S., 2014. Long-period seismicity in the shallow volcanic edifice formed from slow-rupture earthquakes. Nat. Geosci. 7, 71–75.

Belousov, A., Belousova, M., Edwards, B., Volynets, A., Melnikov, D., 2015. Overview of the precursors and dynamics of the 2012–2013 basaltic fissure eruption of Tolbachik Volcano, Kamchatka, Russia. J. Volcanol. Geotherm. Res. 307, 22–37.

Bergal-Kuvikas, O., 2015. Geochemical Studies of Volcanic Rocks from the Northern Part of Kuril–Kamchatka Arc: Tectonic and Structural Constraints on the Origin and Evolution of Arc Magma. PhD thesis. Hokkaido University.

Chebrov, V.N., Droznin, D.V., Kugaenko, Y.A., Levina, V.I., Senyukov, S.L., Sergeev, V.A., Shevchenko, Y.V., Yashchuk, V.V., 2013. The system of detailed seismological observations in Kamchatka in 2011. J. Volcanol. Seismol. 5, 161–170.

Chouet, B., 2003. Volcano seismology. Pure Appl. Geophys. 160 (3–4), 739–788.

Chouet, B.A., 1988. Resonance of a fluid-driven crack: radiation properties and implications for the source of long-period events and harmonic tremor. J. Geophys. Res. 93, 4375–4400.

Chouet, B.A., 1996. Long-period volcano seismicity: its source and use in eruption forecasting. Nature 380 (6572), 309–316.

Chouet, B.A., Matoza, R.S., 2013. A multi-decadal view of seismic methods for detecting precursors of magma movement and eruption. J. Volcanol. Geotherm. Res. 252, 108–175.

Churikova, T.G., Gordeychik, B.N., Ivanov, B.V., Wörner, G., 2013. Relationship between Kamen Volcano and the Klyuchevskaya group of volcanoes (Kamchatka). J. Volcanol. Geotherm. Res. 263, 3–21.

Dorendorf, F., Wiechert, U., Wörner, G., 2000. Hydrated sub-arc mantle: a source for the Kluchevskoy volcano, Kamchatka/Russia. Earth Planet. Sci. Lett. 175, 69–86.

Droznin, D.V., Shapiro, N.M., Droznina, S.Y., Senyukov, S.L., Chebrov, V.N., Gordeev, E.I., 2015. Detecting and locating volcanic tremors on the Klyuchevskoy group of volcanoes (Kamchatka) based on correlations of continuous seismic records. Geophys. J. Int. 203 (2), 1001–1010.

Fedotov, S.A., Jarinov, N.A., Gontovaya, L.I., 2010. The magmatic system of the Klyuchevskaya group of volcanoes inferred from data on its eruptions, earthquakes, deformation, and deep structure. J. Volcanol. Seismol., 1–33.

Fedotov, S.A., Khrenov, A.P., Jarinov, N.A., 1987. Klyuchevskoy volcano, its activity in 1932–1986 and possible development. J. Volcanol. Seismol. 4, 3–16.

Fehler, M., 1983. Observations of volcanic tremor at Mount St. Helens volcano. J. Geophys. Res. 88, 3476–3484.

Frank, W.B., Shapiro, N.M., Husker, A.L., Kostoglodov, V., Gusev, A.A., Campillo, M., 2016. The evolving interaction of low-frequency earthquakes during transient slip. Sci. Adv. 2 (4), e1501616.

Frank, W.B., Shapiro, N.M., Husker, A.L., Kostoglodov, V., Romanenko, A., Campillo, M., 2014. Using systematically characterized low-frequency earthquakes as a fault probe in Guerrero, Mexico. J. Geophys. Res. 119 (10), 7686–7700.

Gibbons, S.J., Ringdal, F., 2006. The detection of low magnitude seismic events using array-based waveform correlation. Geophys. J. Int. 165 (1), 149–166.

Gordeev, E.I., Melnikov, Y.Y., Sinitsin, V.I., Chebrov, V.N., 1986. Volcanic tremor of the Kliuchevskoy volcano (summit eruption in 1984). J. Volcanol. Seismol. 5, 39–53.

Gordeev, E.I., Murav'ev, Y.D., Samoilenko, S.B., Volynets, A.O., Mel'nikov, D.V., Dvigalo, V.N., 2013. The Tolbachik fissure eruption of 2012–2013: preliminary results. Dokl. Earth Sci. 452 (2), 1046–1050.

Gorelchik, V.I., Garbuzova, V.T., Storcheus, A.V., 2004. Deep-seated volcanic processes beneath Klyuchevskoi volcano as inferred from seismological data. J. Volcanol. Geotherm. Res. 6, 21–34.

Han, J., Vidale, J.E., Houston, H., Schmidt, D.A., Creager, K.C., 2018. Deep long-period earthquakes Beneath Mount St. Helens: their relationship to tidal stress, episodic tremor and slip, and regular earthquakes. Geophys. Res. Lett.

Hill, D.P., 1977. A model for earthquake swarms. J. Geophys. Res. 82 (8), 1347–1352.

Iverson, R.M., Dzurisin, D., Gardner, C.A., Gerlach, T.M., LaHusen, R.G., Lisowski, M., Major, J.J., Malone, S.D., Messerich, J.A., Moran, S.C., et al., 2006. Dynamics of seismogenic volcanic extrusion at Mount St. Helens in 2004–2005. Nature 444 (7118), 439–443.

Jolly, A., Lokmer, I., Thun, J., Salichon, J., Fry, B., Chardot, L., 2017. Insights into fluid transport mechanisms at White Island from analysis of coupled very long-period (VLP), long-period (LP) and high-frequency (HF) earthquakes. J. Volcanol. Geotherm. Res. 343, 75–94.

Kendrick, J.E., Lavallée, Y., Hirose, T., Di Toro, G., Hornby, A.J., De Angelis, S., Dingwell, D.B., 2014. Volcanic drumbeat seismicity caused by stick-slip motion and magmatic frictional melting. Nat. Geosci. 7, 438–442.

Konstantinou, K.I., Schlindwein, V., 2003. Nature, wavefield properties and source mechanism of volcanic tremor: a review. J. Volcanol. Geotherm. Res. 119 (1), 161–187.

Koulakov, I., Abkadyrov, I., Al Arifi, N., Deev, E., Droznina, S., Gordeev, E.I., Jakovlev, A., El Khrepy, S., Kulakov, R.I., Kugaenko, Y., et al., 2017. Three different types of plumbing systems beneath the neighboring active volcanoes of Tolbachik, Bezymianny and Klyuchevskoy in Kamchatka. J. Geophys. Res. 122 (5).

Koulakov, I., Gordeev, E.I., Dobretsov, N.L., Vernikovsky, V.A., Senyukov, S., Jakovlev, A., 2011. Feeding volcanoes of the Kluchevskoy group from the results of local earthquake tomography. Geophys. Res. Lett. 38, L09305.

Kugaenko, Y., Titkov, N., Saltykov, V., 2015. Constraints on unrest in the Tolbachik volcanic zone in Kamchatka prior the 2012–2013 flank fissure eruption of Plosky Tolbachik volcano from local seismicity and GPS data. J. Volcanol. Geotherm. Res. 307, 38–46.

Lees, J.M., Gordeev, E.I., Ripepe, M., 2004. Explosions and periodic tremor at Karymsky Volcano, Kamchatka, Russia. Geophys. J. Int. 158 (3), 1151–1167.

Levin, V., Droznina, S., Gavrilenko, M., Carr, M., Senyukov, S., 2014. Seismically active sub-crustal magma source of the Klyuchevskoy volcano in Kamchatka, Russia. Geology 42, 983–986.

Levin, V., Shapiro, N.M., Park, J., Ritzwoller, M.H., 2002. Seismic evidence for catastrophic slab loss beneath Kamchatka. Nature 418, 763–767.

Lowen, S.B., Teich, M.C., 2005. Fractal-Based Point Processes, vol. 366. John Wiley & Sons.

Matoza, R.S., Chouet, B.A., 2010. Subevents of long-period seismicity: implications for hydrothermal dynamics during the 2004–2008 eruption of Mount St. Helens. J. Geophys. Res. 115 (B12).

Matoza, R.S., Shearer, P.M., Okubo, P.G., 2014. High-precision relocation of long-period events beneath the summit region of Kılauea Volcano, Hawaii, from 1986 to 2009. Geophys. Res. Lett. 41 (10), 3413–3421.

McNutt, S.R., 2005. Volcanic seismology. Annu. Rev. Earth Planet. Sci. 32, 461–491.

Moran, S.C., Malone, S.D., Qamar, A.I., Thelen, W.A., Wright, A.K., Caplan-Auerbach, J., 2008. Seismicity associated with renewed dome building at Mount St. Helens, 2004–2005. In: A Volcano Rekindled: The Renewed Eruption of Mount St. Helens, 2004–2006, vol. 1750. U.S. Geol. Surv., Reston, VA, pp. 27–60.

Nakamichi, H., Hamaguchi, H., Tanaka, S., Ueki, S., Nishimura, T., Hasegawa, A., 2003. Source mechanisms of deep and intermediate-depth low-frequency earthquakes beneath Iwate volcano, northeastern Japan. Geophys. J. Int. 154 (3), 811–828.

Neuberg, J.W., Tuffen, H., Collier, L., Green, D., Powell, T., Dingwell, D., 2006. The trigger mechanism of low-frequency earthquakes on Montserrat. J. Volcanol. Geotherm. Res. 153, 37–50.

Nichols, M., Malone, S., Moran, S., Thelen, W., Vidale, J., 2011. Deep long-period earthquakes beneath Washington and Oregon volcanoes. J. Volcanol. Geotherm. Res. 200 (3–4), 116–128.

Ozerov, A.Y., Firstov, P.P., Gavrilov, V.A., 2013. Periodicities in the Dynamics of Eruptions of Klyuchevskoi Volcano, Kamchatka. In: Volcanism and Subduction: The Kamchatka Region, pp. 283–291.

Power, J., Stihler, S., White, R., Moran, S., 2004. Observations of deep long-period (DLP) seismic events beneath Aleutian arc volcanoes; 1989–2002. J. Volcanol. Geotherm. Res. 138 (3–4), 243–266.

Power, J.A., Stihler, S.D., Chouet, B.A., Haney, M.M., Ketner, D.M., 2013. Seismic observations of Redoubt Volcano, Alaska—1989–2010 and a conceptual model of the Redoubt magmatic system. J. Volcanol. Geotherm. Res. 259, 31–44.

Ripepe, M., Poggi, P., Braun, T., Gordeev, E.I., 1996. Infrasonic waves and volcanic tremor at Stromboli. Geophys. Res. Lett. 23, 181–184.

Roman, D.C., Cashman, K.V., 2006. The origin of volcano-tectonic earthquake swarms. Geology 34 (6), 457–460.

Senyukov, S.L., 2013. Forecasting of the Eruptions of Volcanoes Klyuchevskoy and Bezymianny at Kamchatka. Lambert Academic.

Senyukov, S.L., Droznina, S.Y., Nuzhdina, I.N., Garbuzova, V.T., Kozhevnikova, T.Y., 2009. Studies of the activity of Klyuchevskoi volcano by remote sensing techniques between January 1, 2001, and July 31, 2005. J. Volcanol. Seismol. 3, 50–59.

Senyukov, S.L., Nuzhdina, I.N., Droznina, S.Y., Garbuzova, V., Kozhevnikova, T.Y., Sobolevskaya, O.V., Nazarova, Z.A., Bliznetsov, V.E., 2015. Seismic monitoring of the Plosky Tolbachik eruption in 2012–2013 (Kamchatka Peninsula Russia). J. Volcanol. Geotherm. Res. 302, 117–129.

Shapiro, N.M., Droznin, D.V., Droznina, S.Y., Senyukov, S.L., Gusev, A.A., Gordeev, E.I., 2017a. Deep and shallow long-period volcanic seismicity linked by fluid-pressure transfer. Nat. Geosci. 10 (6), 442–445.

Shapiro, N.M., Sens-Schönfelder, C., Lühr, B., Weber, M., Abkadyrov, I., Gordeev, E.I., Koulakov, I., Jakovlev, A., Kugaenko, Y., Saltykov, V., 2017b. Understanding Kamchatka's extraordinary volcano cluster. Eos 98 (7), 12–17.

Shaw, H.R., Chouet, B., 1991. Fractal hierarchies of magma transport in Hawaii and critical self-organization of tremor. J. Geophys. Res. 96, 10191–10207.

Shelly, D.R., Beroza, G.C., Ide, S., Nakamula, S., 2006. Low-frequency earthquakes in Shikoku, Japan, and their relationship to episodic tremor and slip. Nature 442 (7099), 188–191.

Sicali, S., Barbano, M.S., D'Amico, S., Azzaro, R., 2014. Characterization of seismicity at Mt. Etna volcano (Italy) by inter-event time distribution. J. Volcanol. Geotherm. Res. 270, 1–9.

Soubestre, J., Shapiro, N.M., Seydoux, L., de Rosny, J., Droznin, D.V., Droznina, S.Y., Senyukov, S.L., Gordeev, E.I., 2018. Network-based detection and classification of seismovolcanic tremors: example from the Klyuchevskoy volcanic group in Kamchatka. J. Geophys. Res. 123 (1), 564–582.

Sparks, R., Biggs, J., Neuberg, J., 2012. Monitoring volcanoes. Science 335 (6074), 1310–1311.

Thelen, W., West, M., Senyukov, S., 2010. Seismic characterization of the fall 2007 eruptive sequence at Bezymianny volcano, Russia. J. Volcanol. Geotherm. Res. 194, 201–213.

Waite, G.P., Chouet, B.A., Dawson, P.B., 2008. Eruption dynamics at Mount St. Helens imaged from broadband seismic waveforms: interaction of the shallow magmatic and hydrothermal systems. J. Geophys. Res. 113, B02305.
White, R.A., 1996. Precursory deep long-period earthquakes at Mount Pinatubo. In: Newhall, C.G., Punongbayan, R.S. (Eds.), Fire and Mud: Eruptions and Lahars of Mount Pinatubo, Philippines. Univ. of Washington Press, Seattle, pp. 307–326.
Yogodzinski, G.M., Lees, J.M., Churikova, T.G., Dorendorf, F., Woerner, G., Volynets, O.N., 2001. Geochemical evidence for the melting of subducting oceanic lithosphere at plate edges. Nature 409, 500–504.